Published in final edited form as:
J Nucl Cardiol. 2006 November ; 13(6): 821–830.

PET/CT Imaging: Effect of Respiratory Motion on Apparent Myocardial Uptake

Le Meunier Ludovic, **Maass-Moreno Roberto**, **Carrasquillo Jorge**, **Dieckmann William**, and **Bacharach Stephen**
National Institutes of Health, Dept. Nuclear Medicine

Keywords

PET/CT imaging; Attenuation and scatter correction; Fluorine-18; Image artifacts

INTRODUCTION

Combining positron emission tomography (PET) and high speed computerized tomography (CT) provides functional and anatomical information acquired at nearly the same time, usually resulting in accurate registration between the two modalities. The high speed CT data can therefore be used for PET attenuation correction (AC) instead of the traditional germanium-68 rotating rod source, greatly reducing transmission acquisition time (from 3–6 minutes to a few seconds for cardiac scans). Unfortunately, unlike the rotating rod source transmission measurement, the high speed of the CT freezes respiratory motion at a single point in the respiratory cycle. This can produce a mis-registration between the CT data used to perform attenuation correction and the PET emission data which is acquired over many respiratory cycles. There have been several studies showing that this effect can cause artifacts in PET/CT reconstructions in oncology -especially at borders between the lung and soft tissue, such as the liver-lung interface [1–6]. Because the heart also has a lung-soft tissue interface, it would seem likely that there would be similar artifacts in apparent myocardial activity uptake when performing cardiac PET/CT studies. There is little data [7–8] on this effect in PET/CT cardiac imaging. The objective of this study, therefore, was to determine the magnitude of the potential error in observed myocardial activity uptake due to respiratory induced PET-CT mismatch in human cardiac imaging.

MATERIALS AND METHODS

Study population

The study group consisted of 22 subjects (10 females, 12 males; age 43.6±15.1, height 172.8 ±8.3 cm, weight 79.1±21.1 kg). The study was performed under a National Institutes of Health approved protocol. 25 subjects originally entered the protocol, but one was excluded due to scanner malfunction, one due to inadvertent patient motion, and one due to error in following breathing instructions. All patients gave written informed consent. All subjects were chosen from sequential incoming clinical patients already scheduled for PET/CT scans encompassing the torso, without regard to disease. The exclusion criteria were: pregnancy, respiratory

NIH - NMD, Bldg 10, Rm 1C483 Bethesda Maryland 20892, T: 1-301-435-8205, l_le_meunier@yahoo.com

difficulties which might affect breath holding, and age less than 12, due to potential difficulties understanding the instructions required by the protocol.

Patient preparation

After at least four hours of fasting, approximately 555 MBq of fluorine-18 fluorodeoxyglucose (FDG) was injected intravenously, followed by a 60 minute uptake phase. No other tracer was used in the study and no additional FDG was administered beyond that required for their previously scheduled diagnostic PET procedure. Before injection, patients underwent a training session to insure they understood they were to breathe normally (i.e. at their normal resting tidal volume) and could achieve the breathing patterns required by the protocol.

PET/CT and stand alone PET tomograph

The PET/CT tomograph used in this study was a GE Discovery ST [9]. The CT device had 16 rows of detectors (pitch 1.375:1, helical thickness 3.75 mm, table speed 68.75 mm/s, with a rotation speed of 2.5 revolutions/s). The stand alone PET scanner was a GE Advance with three 111 MBq (nominal) ^{68}Ge rotating rod sources (RRS) used for transmission scanning.

Data acquisition

All 22 patients had three sequential whole body CT scans, each acquired at 35 mA (slightly less than one third of the usual 115 mA utilized conventionally at our site), rather than a single whole body CT scan. It has previously been shown that this reduction in mA gives CT scans which are adequate for attenuation correction [10]. Each patient was asked to hold his/her breath at normal end-inspiration for about 10 to 15 seconds (depending on their height) for the first low dose CT scan, then at normal end-expiration for the second CT scan and finally at roughly mid-volume between end-expiration and end-inspiration for the third scan. A low resistance pneumotachometer (ADInstruments – Respiratory Flow Head 300L) was used to monitor and record absolute changes in lung volume with time, and to coordinate the imaging with respect to the respiratory cycle.

FDG emission data were acquired for 5–7 bed positions, typically from the mid-thigh to the base of the skull (716 to 1013 mm coverage, identical to the CT protocol). The acquisition time was 5 minutes per bed position. The data were acquired in 2D mode. During emission imaging the subjects were asked to breathe normally.

Seven of the subjects, who had particularly good cardiac FDG uptake, were also asked to undergo an additional transmission scan (3 minutes per bed position) with a ^{68}Ge rod source on a GE Advance PET system. This scan was acquired immediately after the conclusion of the PET/CT scan. Attenuation correction performed with rotating rod ^{68}Ge sources are thought not to be affected by respiratory motion because the ^{68}Ge transmission scan and the FDG emission scan both take many minutes to acquire, and thus both average many respiratory cycles together. The attenuation data and the emission data are therefore both blurred by respiration in exactly the same way.

It was desired to use the rotating rod transmission data acquired on the GE Advance Scanner to correct the FDG emission acquired on the PET/CT scanner for attenuation. To do so, it was necessary to align the two data sets. Since the CT scan at various phases of the breathing cycle had dramatically different morphology, attempting to align the ^{68}Ge transmission scan and the CT scan might bias the results depending on the phase of the respiratory cycle. To avoid this bias, immediately after the ^{68}Ge transmission acquisition, each of the 7 patients also underwent an additional PET emission acquisition (8 minutes per bed position with no additional FDG injection) on the GE Advance scanner with two bed positions around the level of the heart. These PET-only emission images were collected for the sole purpose of generating the

alignment matrix necessary to align the ^{68}Ge transmission data with the PET/CT emission data. Performing the alignment using the two FDG scans, both of which are averaged over many breathing cycles, would presumably avoid any respiratory related bias in the alignment.

Image processing

The single PET emission data set obtained from the PET/CT were reconstructed either three or four times, as described below.

For all 22 subjects, the three CT data sets were first converted to PET attenuation values resulting in three different CT attenuation correction maps (CTAC). The subgroup of 15 patients who were scanned only on the PET/CT machine (and did not have a rotating rod transmission scan), each had their emission data reconstructed three times, once with each CTAC (OSEM, 2 iterations, 30 subsets, and 6.5 mm post-filter). This produced three attenuation corrected images from the same PET emission data, each reconstructed with a slightly different attenuation correction (AC) - one AC obtained using the CT at end-expiration (CT_{EXPIR}), another using the CT at mid-volume between end-expiration and end-inspiration (CT_{MIDVOL}) and a third using the CT at end-inspiration (CT_{INSPIR}).

For the 7 patients who underwent the additional rotating rod source transmission measurement, the same PET/CT emission data were reconstructed four times, once using each of the three CTACs for attenuation correction as above, and once using the rotating rod data for attenuation correction. The FLIRT image registration package [11], using a mutual information cost function, was used to align the GE Advance FDG emission scan with the PET/CT emission scan. The resulting registration matrix was then used to bring the rotating rod transmission data acquired on the GE Advance scanner into alignment with the FDG emission data from the PET/CT scanner. The PET emission data from the PET/CT was then reconstructed with the attenuation map obtained using the ^{68}Ge rod source on the Advance PET scanner. The computer used to perform this rotating rod reconstruction did not have software to perform iterative reconstructions, and could only perform filtered back-projection reconstructions. To ensure that all the resulting images in this group of 7 subjects were reconstructed identically, the PET/CT emission data were therefore first corrected for attenuation using each of the three CTACs and the rotating rod transmission data, and then reconstructed using filtered back-projection. A Hanning, 4mm cut-off filter was used to match the spatial resolution of the filtered back-projection to that obtained with OSEM. It has been verified that OSEM and filtered back-projection used as described would both give nearly identical mean values within an ROI [12], but the results in the present paper do not depend on this fact, as only paired comparisons of identically reconstructed data are reported here.

Data analysis

Volume of air in the lungs—The pneumotachometer monitored the change in lung volume during the CT scan, and was used to monitor patient response to breathing instructions and to synchronize each scan to the appropriate part of the respiratory cycle. The CT data were used to determine the absolute volume in the lungs for each of the three positions during the breathing cycle (end-inspiration, end-expiration and mid-volume between end-inspiration and end-expiration). This calculation was made by segmenting each voxel in the CT scan at the level of the lungs, into its component air and non-air parts, as has been validated previously [13]. These measurements were used to determine potential correlations between changes in regional cardiac uptake and absolute lung volumes.

Heart motion—From the CT, the relative displacement of the heart was measured between the three CT scans. This 3D motion was measured by recording the x, y and z coordinates of the geometric center of each anatomical region of interest (anterior, lateral, inferior and septal,

as described below) for each of the three CT and then computing the magnitude of the displacement.

Cardiac Uptake—The emission data were reoriented into three short axis (SA) slices (basal, mid-ventricular and apical) plus one additional segment at the apex (figure 1). Each of the three SA slices was then divided into four regions of interest (ROI): anterior, lateral, inferior and septal. These regions plus the apical segment (apex) are shown in figure 1.

The differences in apparent FDG uptake between the three sets of images produced using the three CTACs were first calculated by taking end-expiration as the reference. The end-expiration breathing phase was (somewhat arbitrarily) selected as the reference since more of the respiratory cycle is spent at volumes near end-expiration than elsewhere. The percent difference between each segment was defined as:

$$\Delta_{(i-EXPIR)} = 100 \times (Up_{CTi} - Up_{CTEXPIR}) \mid Up_{CTEXPIR}, \quad \text{Eq. 1}$$

where Up_{CTi} is the measured FDG uptake in the emission images attenuation corrected using the CT_{MIDVOL} or CT_{INSPIR} and $Up_{CTEXPIR}$ is the measured FDG uptake in the emission images attenuation corrected using CT_{EXPIR}. This equation gives the fractional difference in apparent myocardial uptake when the CT at end-inspiration or at the midpoint of the respiratory cycle was used for attenuation correction, compared to the uptake when the CT at end-expiration was used.

The fractional changes described by equation 1 are based on measurement of absolute uptakes. Although such measurements are possible in PET, the standard clinical practice is to first normalize the cardiac uptake in each segment to the uptake in the hottest segment of the entire heart. This normalization also serves to minimize potential global shifts in the data. Such global shifts may occur when applying equation 1 to absolute data, due to differing attenuation values in regions far from the heart, but in the same slice as the heart (e.g. when liver moves in or out of a the slice with respiration). Therefore the data were also analyzed after normalizing each segment to the hottest segment of the entire myocardium. This permitted changes in the pattern of uptake at end-inspiration and at mid-volume between end-inspiration and end-expiration to be computed at each segment – just as they would be computed in an actual clinical setting. The percent difference between the three normalized cardiac uptakes was also calculated using equation 1, except that Up_{CTi} and $Up_{CTEXPIR}$ then represented each subject's normalized uptake.

For the 7 patients who also underwent a rod source transmission, the rod source attenuation corrected PET data were taken as reference, rather than using CT_{EXPIR}. The percent difference between the rod source attenuation-corrected cardiac uptake and that using the three CT-based attenuation-corrections was defined just as in equation 1, but with EXPIR replaced by RRS (the rotating rod source):

$$\Delta_{(i-RRS)} = 100 \times (Up_{CTi} - Up_{RRS}) \mid Up_{RRS}, \quad \text{Eq. 2}$$

where Up_{CTi} is the measured FDG uptake in the emission images attenuation corrected using the CT_{EXPIR}, CT_{MIDVOL} or CT_{INSPIR} and Up_{RRS} is the ^{68}Ge rotating rod source-attenuation corrected uptake (or the corresponding normalized values).

Statistical analyses

Comparisons between uptake of segments, and of cardiac motion, were made by paired Student's t-test (two sided). Non-significant differences were taken as those for which $p>=0.05$.

Tests as to whether correlations were significantly different than 0 were performed assuming the Student's t distribution, using n-2 degrees of freedom.

RESULTS

Heart motion

Consistent with previous reports [14], the heart (and other organs, such as the liver) was displaced between the three CT scans. Figure 2 shows a typical coronal view of the same CT slice of a patient. These two CT scans were taken during normal breathing at end-expiration and at end-inspiration (average change in lung volume compared to end-expiration was 0.52 ± 0.25 L at mid-volume and 1.01 ± 0.54 L at end-inspiration). Taking CT_{EXPIR} as a reference, the average motion of each segment of the heart, over all 22 subjects, is shown in table 1 for the mid-ventricular SA slice.

FDG Uptake

Each of the three CT scans used for attenuation correction showed the heart at a different position in relation to the lungs, liver and other soft tissue. This in turn produced marked changes in apparent global and regional myocardial uptake when each of these CT scans was used to reconstruct the FDG data. Figure 3 illustrates the typical effect of respiratory motion on apparent cardiac uptake. The top row of figure 3 shows the same CT slice at 2 different points in the breathing cycle (end-expiration and end-inspiration). The second row shows one PET emission data set reconstructed twice, using each of the two CT scans in row 1 for attenuation correction. In the 2nd row the same intensity scale is used for both images in order to show global changes in apparent uptake. The FDG image attenuation corrected with the CT at end-expiration (2nd row left) is globally brighter than the end-inspiration corrected image (2nd row right) due to the change of AC. For clinical purposes images are usually normalized to the maximum uptake. Therefore in the 3rd row of figure 3 the same two reconstructed images as in row 2 are shown each scaled to its own maximum. From these images it is clear that using the different CT scans for attenuation correction produces not only global changes (as in the middle row) but also regional changes (e.g. in the 3rd row of figure 3 the two images do not have the same degree of apparent uptake in the lateral wall, shown with arrows).

Fractional changes in apparent absolute global FDG uptake were assessed using an ROI encompassing the entire myocardium (a volume of interest including all segment ROIs for all three slices plus the apex). Compared to the measured uptake when the CT scan at end-expiration was used for attenuation correction ($Up_{CTEXPIR}$), the absolute apparent global cardiac uptake, averaged over all 22 subjects, decreased by 14.7±8.2% for $Up_{CTMIDVOL}$ and 18.0±11.0% for $Up_{CTINSPIR}$ (both $p<0.05$, first row of table 2). This global decrease was correlated with the change in volume of the lung as seen in the upper left hand corner of figure 4 ($r=0.72$, $p<0.05$).

The regional differences in apparent FDG absolute uptake relative to $Up_{CTEXPIR}$ when no normalization is performed are also shown in table 2. All values in the table were significantly different from zero ($p<0.05$). Always arbitrarily taking $Up_{CTEXPIR}$ as reference and using equation 1, the anterior and the lateral regions of the heart showed a greater decrease in apparent uptake than the inferior and septal segments. In the mid slice for example (table 2), $Up_{CTMIDVOL}$ showed a difference of −14.8±12.4% for the anterior region and −14.7±8.5% for the lateral region, while the differences were only −4.5±7.2% and −3.1±4.4% for the inferior and septal regions respectively. This discrepancy between the anterior and the lateral segments, and the inferior and septal segments persists for other slices, and is often even greater for $Up_{CTINSPIR}$ (table 2). Figure 4 shows the correlation between the decrease in apparent uptake and the change in lung volume for the apex, anterior, lateral, inferior and septal segments of

the heart (averaged over the three ventricular slices). As with the global values (upper left hand corner of figure 4), the regional decreases were significantly correlated with the changes in lung volume (all correlations $p<0.05$). The smaller slopes for the inferior and septal sectors compared to the anterior and lateral sectors confirm that respiratory motion can change the pattern of regional uptake.

The % change in apparent cardiac uptake after normalizing each subject's uptake to the sector having the maximum uptake for that patient are shown as a polar map illustration in figure 5. As described previously, the data in figure 5 are expressed relative to a normalized FDG image reconstructed using CT_{EXPIR} for attenuation correction. As with the non-normalized results, the normalized segments shown in figure 5 also showed different apparent decreases in uptake. The anterior and lateral regions – which often have large interfaces with the lung - were more affected by respiration (dark color) than the inferior and septal segments (light color).

In all the above computations, FDG uptake using CT_{EXPIR} for attenuation correction was arbitrarily taken as a reference. Table 3 shows the apparent cardiac uptake when the rotating rod source transmission scan is taken as a reference. Table 3 shows the absolute FDG uptake differences between the rotating rod source corrected data and the data corrected with the three different CT scans. Row 1 of table 3 shows the results of FDG global uptake – i.e. when a region of interest encompassing the entire myocardium was used. As can be seen in table 3, the apparent uptake in the whole heart is reduced considerably when the CT scans were used for AC compared to using the rotating rod source AC. The reduction was minimal for CT_{EXPIR}, but was increasingly larger for CT_{MIDVOL} and CT_{INSPIR}. On a region by region basis, as seen in table 3, the absolute apparent FDG uptake was reduced considerably more in some regions than in others, producing erroneous regional changes in observed uptake. Many of these regional changes were statistically significant at the $p<0.05$ level (see table 3). The polar map in figure 6 shows the same comparisons as table 3 (rotating rod source corrected uptake versus CT corrected FDG uptake), but now each patient's FDG uptake has been normalized to the hottest segment in the heart. As seen in figure 6 the uptake using the ^{68}Ge rotating rod source which appears by definition uniform, becomes successively more non-uniform when CT_{EXPIR}, CT_{MIDVOL} and CT_{INSPIR} were used to perform the attenuation correction. All of these reductions were statistically significant at the $p<0.05$ level.

DISCUSSION

Whether the patient holds or does not hold his breath during the CT scan, a fast CT scan freezes the lungs at one point in the respiratory cycle. Because this CT scan does not duplicate the respiratory blurring inherent in the emission data, using the CT scan to perform attenuation correction may substantially alter the apparent cardiac FDG uptake. The decrease in the global apparent uptake (i.e. averaged over the whole myocardium) when CT_{MIDVOL} or CT_{INSPIR} was used for AC rather than CT_{EXPIR}, is probably due to the fact that at end-expiration the liver appears in many cardiac slices, while at mid-volume and at end-inspiration, more heart slices contain lung rather than liver (e.g. figure 3). This causes the CT_{INSPIR} and CT_{MIDVOL} attenuation correction to under-correct the data compared to the correction using CT_{EXPIR}. Segmental changes, compared to $Up_{CTEXPIR}$, varied from around −2.4% in the septal region for $Up_{CTMIDVOL}$ (apical slice) to −30.2% in the anterior region for $Up_{CTINSPIR}$ (apical slice). The different behavior between the septal and the anterior or lateral regions can be explained by the fact that for the anterior and lateral segments respiratory motion occurs at a lung-tissue interface, while in the septum there is no such interface. Referring to the region of interest drawn on figure 3 (top row, right), at end-inspiration the attenuation correction algorithm will use lung tissue not soft tissue in the anterior and lateral walls of the myocardium, and will erroneously do less attenuation correction. This causes the PET image attenuation corrected using CT_{EXPIR} to appear less bright than these regions on the image corrected using

CT_{INSPIR} (figure 3 middle and bottom rows). This does not occur at the septal (and inferior) wall.

When $Up_{CTEXPIR}$ was used as the standard, the magnitude of the global and regional changes were correlated with the absolute change in lung volume (figure 4) indicating that, as expected, the larger the change in volume, the larger the effect on apparent FDG uptake. Even when the cardiac uptake was normalized (i.e. each patient's cardiac scan normalized to the hottest sector for that patient), the erroneous regional changes (with $Up_{CTEXPIR}$ taken as the standard) persisted, as shown in figure 5. Presumably such respiratory caused regional changes would introduce errors into clinical readings.

The differences between $Up_{CTEXPIR}$ and both $Up_{CTINSPIR}$ and $Up_{CTMIDVOL}$ were larger than expected. Since it was not certain that the attenuation correction using the CT_{EXPIR} was the true correction, a subset of subjects was analyzed using a ^{68}Ge rotating rod source as the reference method of attenuation correction. This rod source rotates around the subject for many minutes averaging together many respiratory cycles. Similarly, the FDG emission images also are acquired over many respiratory cycles. Therefore the ^{68}Ge rotating rod source should best match the circumstances under which the FDG emission data were acquired, and would presumably be the most accurate method of attenuation correction in terms of respiratory motion. When the uptake with the rotating rod source (Up_{RRS}) was used as the standard, the cardiac uptake reconstructed with CT_{EXPIR} produced the smallest non-uniformities whether the data were un-normalized (table 3) or whether each segment was normalized to the hottest segment (figure 6). CT_{MIDVOL} and CT_{INSPIR} produced larger erroneous regional changes than CT_{EXPIR}. Again the free wall behaved very differently than the septal wall. For example in the mid-ventricular slice of $Up_{CTINSPIR}$ (figure 6) the lateral segment was depressed over 30% while the septum was depressed only 10%.

Note that despite the normalization, none of the segments was unity. This is because all patients were averaged together, and different segments were the "hottest" for different patients.

The clinical impact of these respiratory non-uniformities will depend on the application. If a sector value of a normal segment were being compared to a normal database, respiratory effects might make that sector closer to the abnormal limit. The clinical significance of this effect will depend on whether or not the normal database variability was large compared to the corresponding value in figure 6. Normal database variability in turn may depend on the pharmaceutical, the sector, and the details of how the database was implemented. One might speculate that were the CT acquired at mid-volume or end-inspiration, the clinical effect would be large.

Many potential solutions have been suggested to correct the bias introduced by the high speed CT attenuation correction. First, CT and PET can be respiratory gated [15–16]. But this method is difficult to perform and it can greatly increase acquisition times. Another solution recently suggested is to use a cine CT which is available on most of the machines. The idea is to acquire multiple phases of the breathing cycle and to average all the phases together. One then creates a respiratory blurred CT which matches the blurring of a rod source transmission [17]. In theory, this method should give identical results to the rotating rod source. However increased radiation dose may be a limitation of this method unless beam current is reduced substantially. Another solution would be to manually register the CT data to the emission data prior to performing attenuation correction, although there may be no single point in the respiratory cycle for which the CT data exactly match the respiratory blurred emission data. Alternatively, a very low current, slow CT scan could be used to average many respiratory cycles together during the acquisition. This would come close to duplicating the rotating rod. However at the moment,

not all CT scanners are able to scan sufficiently slowly, at low enough beam currents, and at slow speeds respiratory reconstruction artifacts could occur in the CT data itself.

CONCLUSION

PET/CT shows great promise for cardiac imaging. However, the data above show that there can be a respiratory motion mismatch between the PET data and the CT data used to correct the PET for attenuation. As shown above, this mismatch may lead to significant errors in both apparent and regional cardiac uptake. The mismatch appears smallest when end-expiratory CT images are used, but even in that case may well be clinically important. Many methods have the potential to reduce this mismatch. It is clear that these methods must be explored and ultimately applied. Simply ignoring the problem appears to lead to the production of significant erroneous regional defects.

References

1. Beyer T, Antoch G, Blodgett T, Freudenberg LF, Akhurst T, Mueller S. Dual-modality PET/CT imaging: the effect of respiratory motion on combined image quality in clinical oncology. Eur J Nucl Med Mol Imaging 2003 Apr;30(4):588–96. [PubMed: 12582813]
2. Goerres GW, Burger C, Kamel E, Seifert B, Kaim AH, Buck A, et al. Respiration-induced attenuation artifact at PET/CT: technical considerations. Radiology 2003 Mar;226(3):906–10. [PubMed: 12616024]
3. Goerres GW, Kamel E, Heidelberg TNH, Schwitter MR, Burger C, von Schulthess GK. PET-CT image co-registration in the thorax: influence of respiration. Eur J Nucl Med Mol Imaging 2002 Mar;29(3): 351–60. [PubMed: 12002710]
4. Osman MM, Cohade C, Nakamoto Y, Wahl RL. Respiratory motion artifacts on PET emission images obtained using CT attenuation correction on PET-CT. Eur J Nucl Med Mol Imaging 2003 Apr;30(4): 603–6. [PubMed: 12536242]
5. Erdi YE, Nehmeh SA, Pan T, Pevsner A, Rosenzweig KE, Mageras G, et al. The CT motion quantitation of lung lesions and its impact on PET-measured SUVs. J Nucl Med 2004 Aug;45(8):1287–92. [PubMed: 15299050]
6. Nakamoto Y, Chin BB, Cohade C, Osman M, Tatsumi M, Wahl RL. PET/CT: artifacts caused by bowel motion. Nucl Med Commun 2004 Mar;25(3):221–5. [PubMed: 15094438]
7. Chin BB, Nakamoto Y, Kraitchman DL, Marshall L, Wahl R. PET-CT evaluation of 2-deoxy-2-[18F] fluoro-D-glucose myocardial uptake: effect of respiratory motion. Mol Imaging Biol 2003 Mar–Apr; 5(2):57–64. [PubMed: 14499145]
8. Koepfli P, Hany TF, Wyss CA, Namdar M, Burger C, Konstantinidis AV, et al. CT attenuation correction for myocardial perfusion quantification using a PET/CT hybrid scanner. J Nucl Med 2004 Apr;45(4):537–42. [PubMed: 15073247]
9. Bettinardi V, Danna M, Savi A, Lecchi M, Castiglioni I, Gilardi MC, et al. Performance evaluation of the new whole-body PET/CT scanner: Discovery ST. Eur J Nucl Med Mol Imaging 2004 Jun;31(6): 867–81. [PubMed: 14770270]
10. Kamel E, Hany TF, Burger C, Treyer V, Lonn AHR, von Schulthess GK, et al. CT vs 68Ge attenuation correction in a combined PET/CT system: evaluation of the effect of lowering the CT tube current. Eur J Nucl Med Mol Imaging 2002 Mar;29(3):346–50. [PubMed: 12002709]
11. Fischer B, Modersitzki J. FLIRT: A flexible image registration toolbox. LECT NOTES COMPUT SC 2003;2717:261–70.
12. Riddell C, Carson RE, Carrasquillo JA, Libutti SK, Danforth DN, Whatley M, et al. Noise reduction in oncology FDG PET images by iterative reconstruction: a quantitative assessment. J Nucl Med 2001 Sep;42(9):1316–23. [PubMed: 11535719]
13. Mullan BF, Galvin JR, Zabner J, Hoffman EA. Evaluation of in vivo total and regional air content and distribution in primate lungs with high-resolution CT. Acad Radiol 1997 Oct;4(10):674–9. [PubMed: 9344289]

14. Huesman RH, Klein GJ, Reutter BW, Botvinick EH, Budinger TF. Evaluation of respiratory compensation efforts in cardiac PET. J Nucl Med 2000 May;41(5):79.

15. Nehmeh SA, Erdi YE, Pan T, Pevsner A, Rosenzweig KE, Yorke E, et al. Four-dimensional (4D) PET/CT imaging of the thorax. Med Phys 2004 Dec;31(12):3179–86. [PubMed: 15651600]

16. Nehmeh SA, Erdi YE, Pan T, Yorke E, Mageras GS, Rosenzweig KE, et al. Quantitation of respiratory motion during 4D-PET/CT acquisition. Med Phys 2004 Jun;31(6):1333–8. [PubMed: 15259636]

17. Pan TS, Mawlawi C, Nehmeh SA, Erdi YE, Luo DS, Liu HH, et al. Attenuation correction of PET images with respiration-averaged CT images in PET/CT. J Nucl Med 2005 Sep;46(9):1481–7. [PubMed: 16157531]

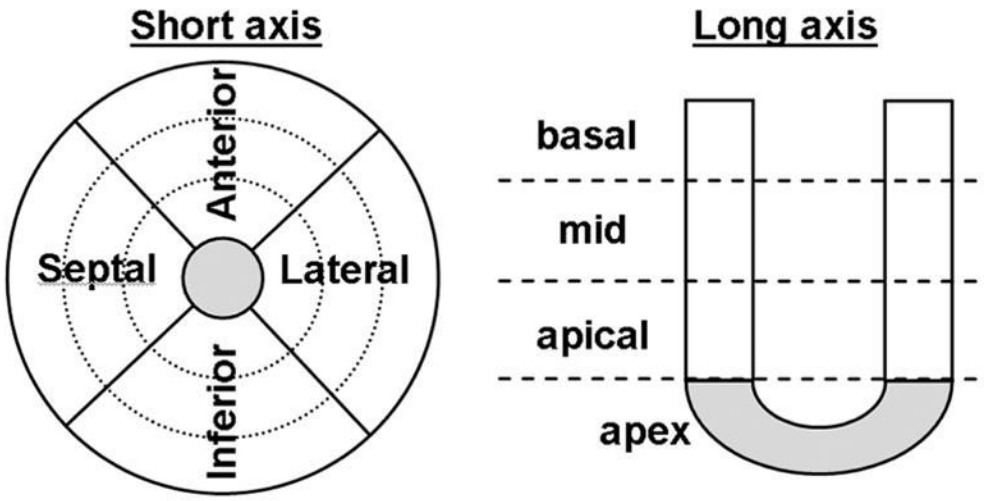

Figure 1.
Reorientation in short axis view. The heart was divided in 3 ventricular slices (basal, mid, apical) plus the apex. Each slice was then divided into 4 sectors (anterior, inferior, lateral and septal).

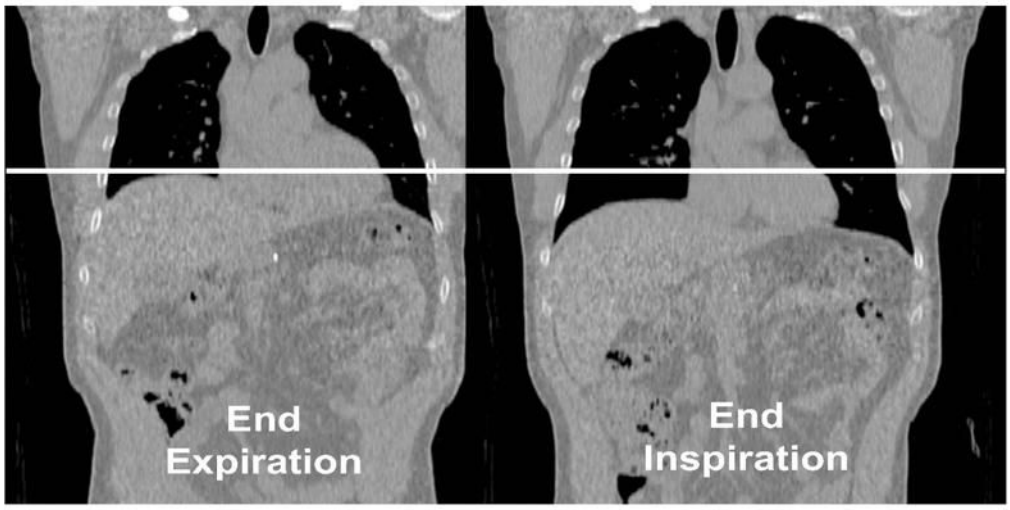

Figure 2.
coronal view of the same CT slice taken at normal end-expiration (left) and at normal end-inspiration (right). The white line shows the magnitude of the motion of the heart and other structures.

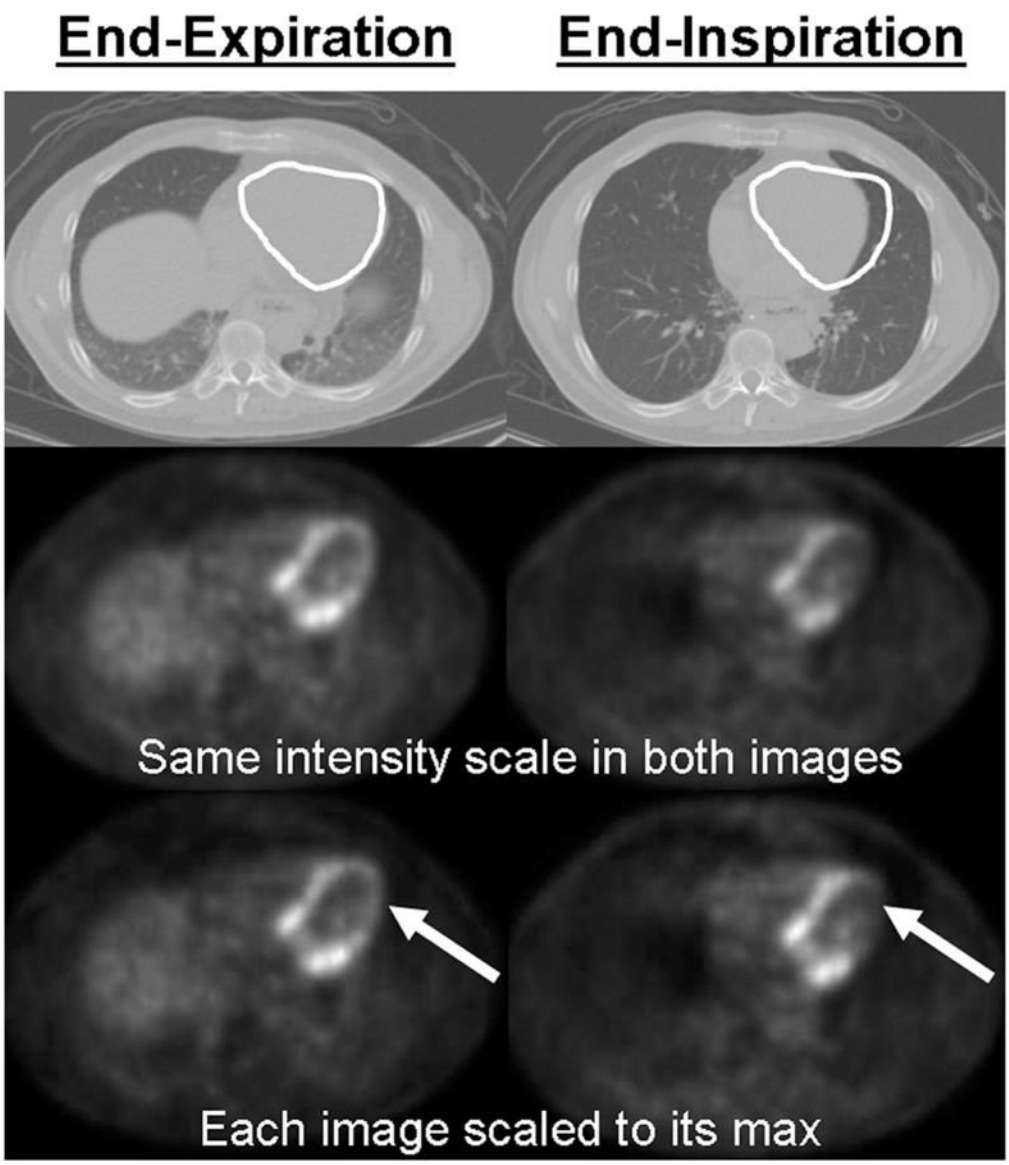

Figure 3.

illustration of the global and regional uptake changes due to the difference between the attenuation maps. Top row: white ROI on the CT shows the magnitude of the heart motion. 2nd row: The same PET emission data reconstructed using the 2 CTs shown in the first row for attenuation correction. These images are displayed with the same intensity scale to illustrate the global uptake change between the 2 images (the image attenuation corrected with the end-expiration CT is globally brighter). 3rd row: The same two images as in the 2nd row but with each image scaled to its max in order to show local uptake changes. The arrows indicate that a large change in regional uptake has occurred between images reconstructed using CT_{EXPIR} (left) and CT_{INSPIR} (right) for attenuation correction.

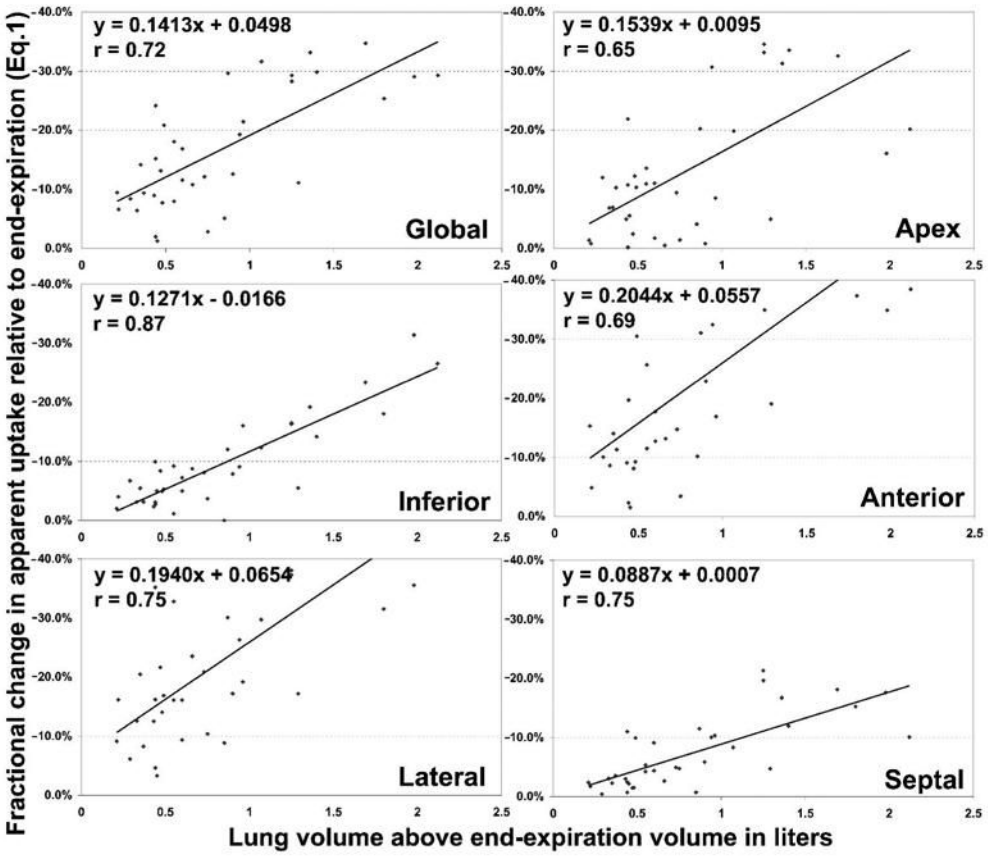

Figure 4.

Correlation between % change in apparent uptake (equation 1) with change in lung volume, using the cardiac uptake attenuation corrected with the end-expiration CT ($Up_{CTEXPIR}$) as a reference. Upper left corner: global results; remaining graphs showing each of the 4 segment's correlation with change in lung volume, averaged over the 3 ventricular slices, and also the correlation with the apex.

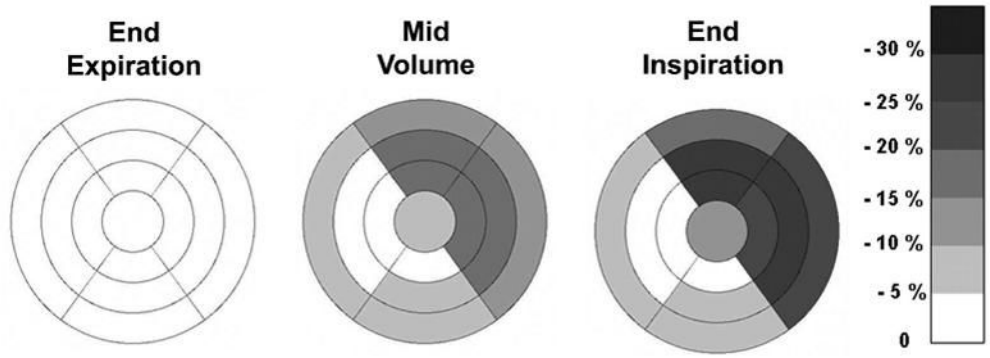

Figure 5.

Polar map showing the regional differences between (normalized) apparent cardiac uptake of PET data attenuation corrected with the CT_{INSPIR} or CT_{MIDVOL} scans, compared to the uptake obtained from the same PET data in which the CT_{EXPIR} was used for attenuation correction (darker color corresponding to greater % difference). Negative values imply a reduction in apparent normalized activity. PET data corrected with the end-expiration CT shows uniform uptake by definition (equation 1).

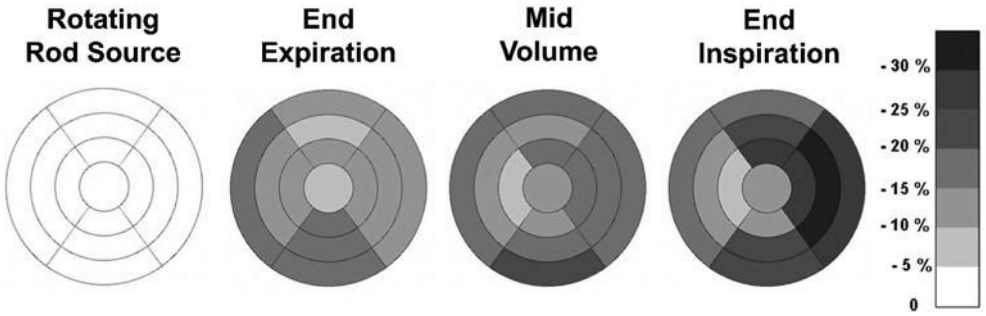

Figure 6.

Polar map showing the regional differences between (normalized) apparent cardiac uptake of PET data attenuation corrected with the 3 CT scans, compared to the uptake obtained from the same PET data in which the ^{68}Ge rotating rod source (RRS) was used for attenuation correction (darker color corresponding to greater % difference). Negative values imply a reduction in apparent normalized activity. PET data corrected by the RRS shows uniform uptake by definition (equation 2).

Table 1

Magnitude of the heart motion (in mm) taking the CT at end-expiration (CT_{EXPIR}) as reference. Mid-ventricular slice, averaged over all 22 subjects.

Mean Displacement (mm) Relatively to CT_{EXPIR}	**CT_{MIDVOL}**	**CT_{INSPIR}**
Apex	11.6±2.3	18.1±6.2
Mid-ventricular SA		
Anterior	6.8±1.0	14.3±2.5
Lateral	6.9±3.1	13.0±2.5
Inferior	8.3±2.9	12.6±3.6

All $p<0.05$

Table 2

Global and regional apparent uptake differences (using equation 1) between the three CT attenuation corrected cardiac uptakes. The cardiac uptake computed using the end-expiration CT ($Up_{CTEXPIR}$) is the reference. Negative signs imply the value is lower than for $Up_{CTEXPIR}$.

Regional Uptake Bias (%)$Up_{CTEXPIR}$ as reference	**$Up_{CTMIDVOL}$**	**$Up_{CTINSPIR}$**
Global	−14.7 ± 8.2	−18.0 ± 11.0
Apex	−8.3 ± 6.3	−16.8 ± 14.2
Apical slice		
Anterior	−17.6 ± 17.5	−30.2 ± 23.6
Inferior	−2.9 ± 5.7	−7.9 ± 8.5
Lateral	−14.1± 12.4	−25.5 ± 17.6
Septal	−2.4 ± 5.7	−7.1 ± 8.3
Mid slice		
Anterior	−14.8 ± 12.4	−26.7 ± 19.5
Inferior	−4.5 ± 7.2	−11.9 ± 9.8
Lateral	−14.7 ± 8.5	−29.0 ± 15.2
Septal	−3.1 ± 4.4	−8.1 ± 7.7
Basal slice		
Anterior	−10.3 ± 7.2	−18.4 ± 13.5
Inferior	−6.7 ± 7.0	−13.2 ± 10.4
Lateral	−12.3 ± 7.8	−24.4 ± 13.6
Septal	−5.1 ± 4.9	−9.3 ± 7.2

All $p<0.05$

Table 3

Global and regional differences between cardiac uptake using the ^{68}Ge rod source for attenuation correction (Up_{RRS}) and the uptake computed using the three CT scans (equation 2). Negative values imply a value less than that obtained with the rotating rod source.

Regional Uptake Bias (%) Up_{RRS} as reference	**$Up_{CTEXPIR}$**	**$Up_{CTMIDVOL}$**	**$Up_{CTINSPIR}$**
Global	−5.9 ± 8.2 (NS)	−12.3 ± 10.0	−22.8 ± 11.2
Apex	−1.5 ± 6.9 (NS)	−7.4 ± 13.7	−15.1 ± 16.4
Apical slice			
Anterior	−3.0 ± 21.1 (NS)	−14.5 ± 27.3 (NS)	−32.5 ± 24.8
Inferior	−8.6 ± 11.4 (NS)	−7.8 ± 2.9	−14.0 ± 9.6
Lateral	−3.8 ± 19.2 (NS)	−13.8 ± 17.0 (NS)	−30.5 ± 21.6
Septal	−6.3 ± 6.7	−5.0 ± 7.8 (NS)	−11.9 ± 7.4
Mid slice			
Anterior	−1.2 ± 18.1 (NS)	−9.1 ± 22.2 (NS)	−28.1 ± 20.0
Inferior	−10.0 ± 7.3	−16.3 ± 4.1	−21.5 ± 11.2
Lateral	−2.1 ± 18.5 (NS)	−11.6 ± 13.2	−32.5 ± 19.0
Septal	−7.9 ± 5.6	−7.9 ± 3.9	−13.2 ± 7.4
Basal slice			
Anterior	−2.5 ± 9.5 (NS)	−13.3 ± 13.3	−22.1 ± 16.5
Inferior	−12.4 ± 7.9	−21.3 ± 10.6	−23.0 ± 12.3
Lateral	−2.9 ± 10.7 (NS)	−14.8 ± 12.9	−28.9 ± 15.1
Septal	−11.4 ± 5.7	−15.6 ± 7.1	−16.4 ± 8.7

All $p<0.05$ except when specified not significant (NS)